

## Calibration of the Au labeling technique to measure vacancy defects in Si

R. Kalyanaraman and T. E. Haynes

*Solid State Division, Oak Ridge National Laboratory, Oak Ridge, Tennessee 37831*

V. C. Venezia, D. C. Jacobson, H.-J. Gossmann and C. S. Rafferty

*Bell Laboratories, Lucent Technologies, Murray Hill, NJ 07974*

### ABSTRACT

It has been shown recently that Au labeling can be used to profile vacancy-type defects located near half the projected range ( $\frac{1}{2}R_p$ ) in MeV-implanted Si. In this work we have quantified the technique by determining the ratio of vacancies annihilated to Au atoms trapped (calibration factor ' $k$ ') for the Au labeling technique. The 3 step experiment involved 1) a high-energy Si-self implant (HEI) followed by an anneal to form stable vacancy clusters, 2) a controlled removal of vacancies via a medium energy Si self implant and interstitial-cluster dissolution anneal, and finally 3) Au labeling to count the change in vacancy concentration in the near surface region (0.1-1.6 $\mu$ m). It is seen that the Au concentration decreases linearly with increasing interstitial injection and the slope of this decrease determined the number of vacancies per trapped Au atom. The value of  $k$  was determined to be  $1.2 \pm 0.2$  vacancies per trapped Au atom.

### INTRODUCTION

Ion implantation as a processing step in Si device fabrication has resulted in extensive research into the study of defects in Si. This has mainly been due to the supersaturation of point defects invariably accompanying ion implantation and the subsequent defect evolution. In the past decade large advances have been made in correlating defect evolution with dopant diffusion and device behavior [1, 2]. For instance, the direct influence of the interstitial-type {311} rod-like defects [1] on the transient enhanced diffusion of B showed how critical it was to understand the evolution from point to extended defects and finally to dissolution of ion implanted defects. Recently, Holland and co-workers [3] showed from transmission electron microscopy (TEM) studies that extended vacancy-type defects form in the near-surface region for extremely high-dose implants. Other groups have also observed vacancy-type defects under more moderate implantation doses by techniques like x-ray diffraction strain measurements [4], positron annihilation spectroscopy (PAS) S-parameter measurements [5] and x-ray diffuse scattering measurements [6]. While all these techniques are capable of detecting vacancy-type defects, considerable work needs to be done to use them to quantitatively measure the size and distribution of vacancy-type defects.

In the past few years the process of metal gettering to vacancy-type defects has been studied by a number of authors [7,8]. In fact, Venezia and co-workers [9] have used Au to label the vacancy-type defects formed by high-energy Si self implants. In this work, we present experiments designed to obtain the relation between the true vacancy concentration and the Au concentration, given by the calibration factor " $k$ ", using the Au labeling technique [9]. The calibration factor was determined via a 3 step experiment: 1) The vacancy concentration was generated via high-energy ion implantation (HEI) in Si which results in a higher average forward momentum of recoiled atoms produced in the collision cascades producing an excess of vacancy-type defects in the shallow part of the implant profile [10], 2) controlled removal of vacancies was effected by annihilating them with a known number of interstitials from a medium-energy Si

self-implant (+I implant) and 3) Au labeling was carried out to determine the change in vacancy concentration as a function of the injected interstitials (+I). The results of this experiment give for the first time a quantitative profile of vacancy-type defects in high-energy ion implanted Si and consequently, a quantitative understanding of the evolution of vacancy-type defects is now possible.

## EXPERIMENTAL DETAILS

The schematic of the 3-step experiment is shown in figure 1. P-type float-zone Si(100) ( $\rho = 65\text{-}80 \text{ }\Omega\text{-cm}$ ) wafers were implanted with 2-MeV Si (projected range  $R_p \sim 2\text{ }\mu\text{m}$ ) with a dose of

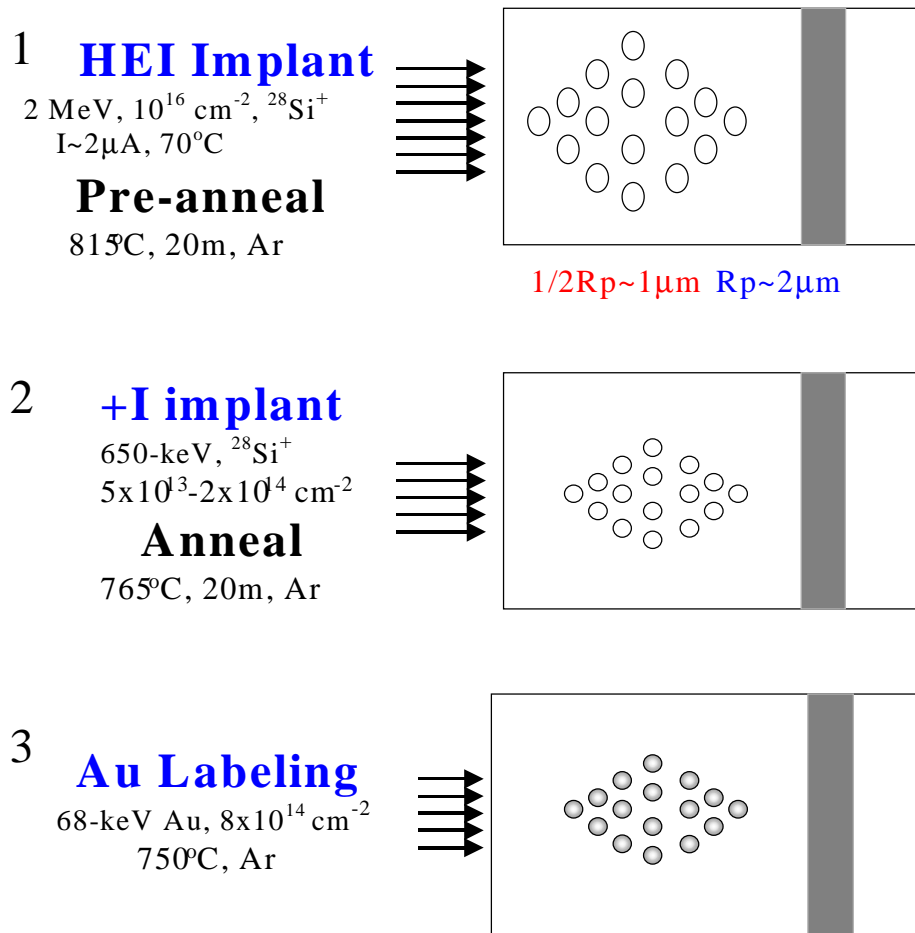


Figure 1. Schematic of the 3-step experiment to determine the calibration factor of the Au labeling technique. Step 1 is the high-energy implant and anneal (HEI) to form stable vacancy clusters. Step 2 is the controlled removal of vacancies by the +I (650-keV) Si implant and anneal. The 3<sup>rd</sup> and final step is Au labeling.

$1 \times 10^{16} \text{ cm}^{-2}$  at an angle of  $7^\circ$  from the surface normal direction using a 1.7 MeV National Electrostatics tandem Pelletron. The substrate temperature during the implant was maintained at  $70\text{-}80^\circ\text{C}$  (to suppress amorphization), while the chamber pressure was between  $2\text{-}5 \times 10^{-6}$  Torr. The HEI samples were then furnace annealed at  $815^\circ\text{C}$  for 20 min in 1 atm of argon

to form stable vacancy-type defects [9]. Following this, the +I interstitial injection was carried out by implanting 600-keV Si<sup>+</sup> ions at doses from  $5 \times 10^{13} \text{ cm}^{-2}$  -  $20 \times 10^{13} \text{ cm}^{-2}$  followed by a 765°C, 20-min anneal in flowing Ar. The R<sub>p</sub> of this implant is ~0.9μm (from SRIM-2000<sup>11</sup>), which puts it almost at ½R<sub>p</sub> of the 2-MeV Si<sup>+</sup> implant. In the third and last step, Au labeling was carried out by implanting Au at 68 keV (R<sub>p</sub>~0.03μm) and  $8 \times 10^{14} \text{ cm}^{-2}$  dose in the HEI samples and the HEI+I samples (i.e. the HEI samples which had the +I implant and anneal). The implanted Au was diffused in at 750°C in 1 atm of argon for times up to 30 h. The Au concentration profiles were then measured by RBS in random geometry, using 2.8 MeV <sup>4</sup>He<sup>2+</sup> at an incident angle of 22° relative to the surface normal direction with the detector at 170° from the incident ion direction.

## DISCUSSION

The presence of vacancy-type defects after the HEI implant and anneal was first confirmed by implanting {311}-defect forming doses of Si near half the projected range (½R<sub>p</sub>) of the HEI implant (R<sub>p</sub> ~2μm). Figure 2 shows the suppression of {311} defect formation for a 600-keV,  $2 \times 10^{14} \text{ cm}^{-2}$  Si self-implant (+I implant) in the HEI sample (fig. 2b), as compared to the defects clearly visible (fig. 2a) after implantation and anneal into a bare-Si wafer. This indicates recombination of the added interstitials from the 600-keV implant with the excess vacancies from the HEI. The features visible near the surface are dislocation loops formed by a separate 50-keV,  $10^{15} \text{ cm}^{-2}$  Si implant (and 800°C, 1hr anneal) prior to the +I implant, which was used to detect the presence of escaping interstitials, if any, from the +I implant [12]. The recombination of interstitials in the vacancy-rich region was also reflected in the Au signal as seen following Au labeling. Figure 3 shows a typical RBS plot comparing the Au concentration after 20 hrs of Au drive-in for the HEI sample (no +I implant) and the HEI sample with a  $2 \times 10^{14} \text{ cm}^{-2}$  +I implant. A number of features are immediately visible from the figure, like the Au surface peak, the Au peak between 0.1-0.3μm labeled 'shoulder', the apparent depletion in Au in the region between 0.3-0.5μm and Au in the region between 0.5-1.6μm. The properties of the shoulder Au and the reasons for the depleted Au are discussed in more detail elsewhere in these proceedings [13]. In this work, the Au in the region between 0.5-1.6μm, referred to as the "½R<sub>p</sub> Au," will be used to determine the calibration factor.

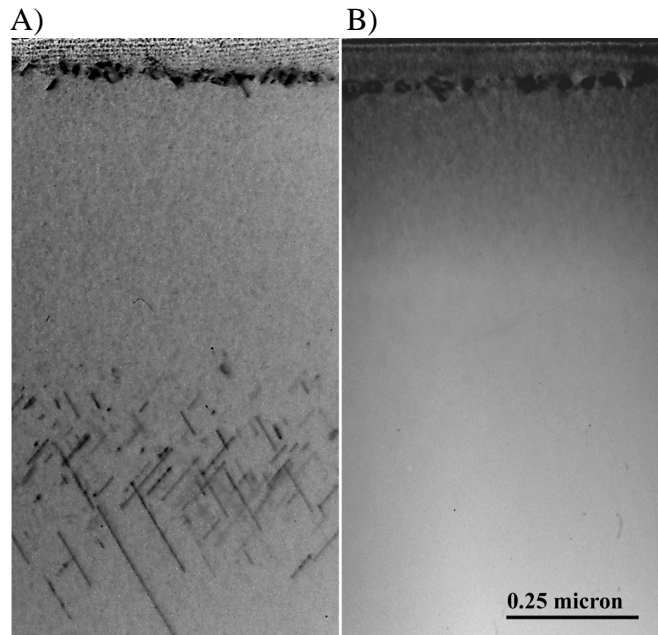


Figure 2) Suppression of extended interstitial defects of {311}-type in a sample containing the HEI implant and anneal (fig 2b) as compared to the implant into a bare-Si wafer (fig 2a) where the defects are clearly visible. 600-keV,  $2 \times 10^{14} \text{ cm}^{-2}$  Si was implanted and annealed at 765°C, 20m to form the {311} defects.

As seen in figure 3, the Au concentration in the  $\frac{1}{2}R_p$  region is clearly different for the two samples. One important observation during the Au drive-in was that the Au concentration took considerable time to saturate. Since the measurement of the calibration factor depends on the amount of Au in the  $\frac{1}{2}R_p$  region, it was necessary to make sure that the measured Au concentration was indeed the stable value. The saturation and stability of Au is more clearly seen in figure 4, where the Au concentration in the  $\frac{1}{2}R_p$  region is plotted as a function of Au drive-in time for samples containing various amounts of +I in the HEI. As is seen clearly, it takes considerable time to saturate, but once saturated, the Au concentration remains stable. Therefore, to obtain reproducible and complete trapping of Au it was first necessary to saturate the Au in all the samples.

Since the suppression of extended interstitial defects (fig. 2b) also corresponded to a decrease in amount of trapped Au (fig. 3), this implied that Au was profiling vacancy-type defects. Thus, a controlled removal of vacancies was effected by varying the dose of the +I implant and detected by Au labeling. The saturated concentration of Au was integrated over the  $\frac{1}{2}R_p$  region and plotted as a function of the +I implanted dose to obtain the variation in Au concentration as a function of

the injected Si ions. The obtained variation is plotted in fig. 5. The observed linear variation indicates a monotonic and proportional decrease in Au concentration with increasing +I dose.

The slope of the integrated Au concentration vs. +I of  $0.85 \pm 15\%$  gives the reduction in number of Au atoms trapped in the vacancy-rich region by the introduction of 1 Si atom. In other words, the inverse of this slope gives the number of vacancies for every trapped Au atom, i.e. the  $k$  factor. This, as shown in figure 5, is  $k \sim 1.2 \pm 0.2$ , indicating that there are approximately 1.2 vacancies for every trapped Au atom. Thus the vacancy concentration can be directly obtained after Au labeling by multiplying the observed Au concentration by a factor of 1.2, provided that the saturated Au concentration is used. Also

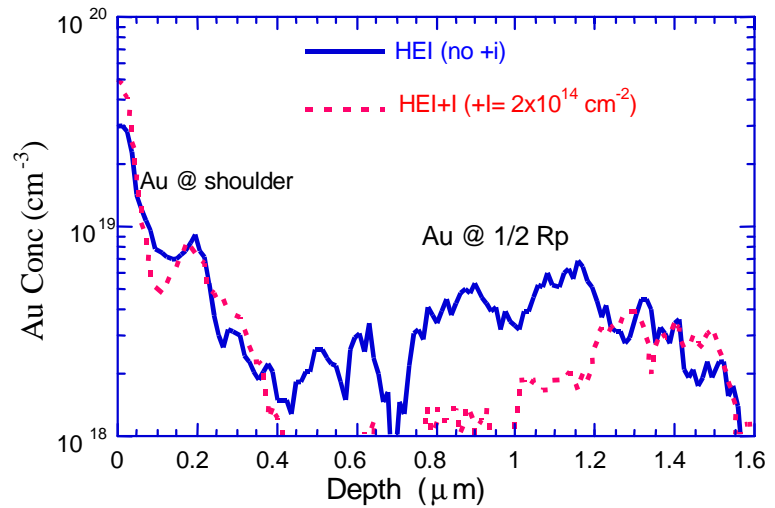


Figure 3) RBS after Au labeling comparing the HEI sample (solid line) with HEI+I (+I= $2 \times 10^{14} \text{ cm}^{-2}$ ) after saturation of Au.

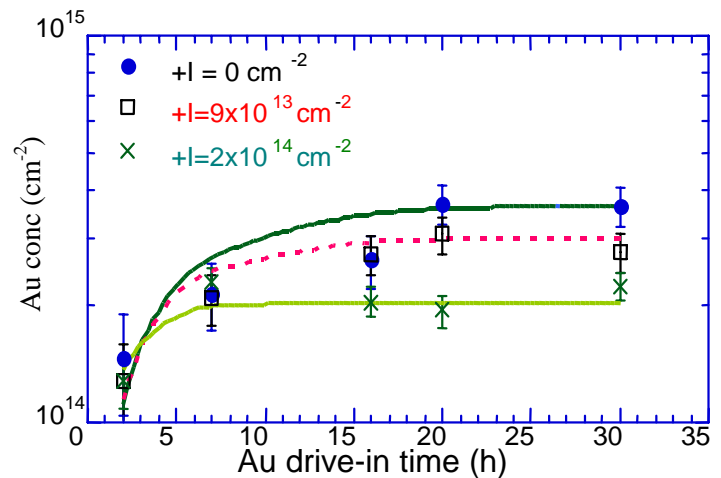


Figure 4) Saturation of Au at  $\frac{1}{2}R_p$  as a function of Au drive-in time for HEI sample with various +I doses. The +I=0 is the sample with only HEI.

plotted in fig. 5 is the saturated Au concentration obtained by exponential  $C_0(1-\exp(-t/\tau))$  fitting of the curves in fig. 4, where  $C_0$  and  $\tau$  are the fit values of saturated concentration and saturation time respectively. The slope using values of  $C_0$  is 0.80, similar to that obtained from the experimental points after 20 hrs of Au drive-in. This confirmed that 20 hrs was sufficient to saturate the sample with the largest Au concentration, i.e. the HEI without +I. Thus the value obtained after 20-hrs of drive-in is a reliable measurement of  $k$ .

## CONCLUSION

A number of checks were performed to determine that all the injected +I Si atoms were confined to the vacancy rich region of the HEI. The results of these checks, appearing in [12] clearly confirm the validity of the measured calibration factor. Further the measured value also indicates that the Au and vacancy-type defect interaction is more likely a volume filling-type of interaction rather than a surface coating-type process, as has been observed in some cases [14]. This difference may be attributed to the fact that the size of the voids and the drive-in conditions are different. While the results of this work are independent of the mechanism, we are currently working on understanding this strong interaction between Au and the vacancy-type defects. Thus, now it is possible to measure the true concentration of stable vacancy-type defects in Si using the Au labeling technique. There seems no apparent hurdle in extending this technique to measure stable vacancy-type defects produced by other processing steps that can lead to supersaturation of vacancies. The only limitation to this technique appears to be the long times and high temperatures required for the drive-in.

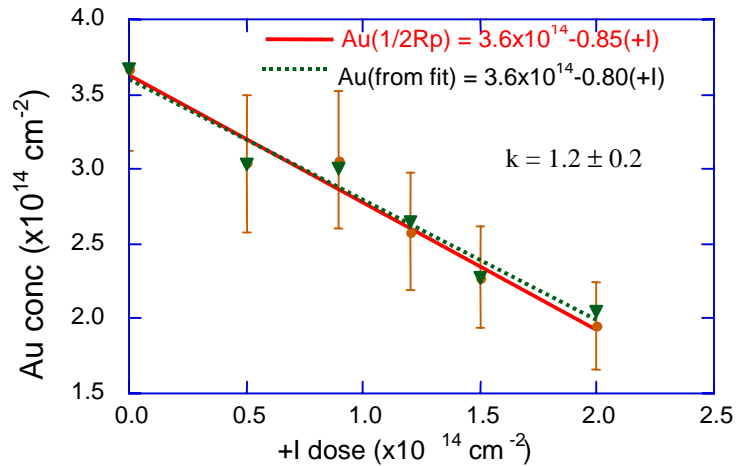


Figure 5) The calibration factor obtained from the inverse of the slope of the integrated Au conc. at  $\frac{1}{2}R_p$  vs. the +I dose after 20 hrs drive-in. Also shown is the fit (triangles) of the saturation curves of fig. 4.

## ACKNOWLEDGEMENT

RK would like to thank Dave Eaglesham, whose idea was the basis for this work and George Gilmer and Janet Benton for stimulating discussions. Research performed at Oak Ridge National Laboratory was sponsored by the U.S. Department of Energy, Office of Science, Laboratory Technology Research Division and the Division of Materials Sciences under contract DE-AC05-00OR22725 with UT-Battelle, LLC.

## REFERENCES

---

1. D.J.Eaglesham, P.A.Stolk, H.-J.Gossmann, J.M.Poate, App. Phys. Lett. **65**, 2305 (1994).
2. J.Y.Cheng, D.J.Eaglesham, D.C.Jacobson, P.A.Stolk, J.L.Benton, J.M.Poate, J. Appl. Phys. **80**, 2105 (1996).
3. O.W.Holland, L.Xie, B.Nielsen, D.S.Zhou, J. Elec. Mat. **25**, 99 (1996).
4. S.L.Ellingboe, and M.C.Ridgway, Nucl. Instrum. Meth. Phys. Res. B **127/128**, 90 (1997).
5. C.Szeles, B.Nielsen, P.Asoka-Kumar, K.G.Lynn, M.Anderle, T.P.Ma, G.W.Rubloff, J. Appl. Phys. **76**, 3403 (1994).
6. M.Yoon, B.C.Larson, J.Z.Tischler, T.E.Haynes, J.-S.Chung, G.E.Ice, P.Zschack, Appl. Phys. Lett. **75**, 2791 (1999).
7. R.A.Brown, O.Kononchuk, G.A.Rozgonyi, S.Koveshnikov, A.P.Knights, P.J.Simpson, F.Gonzalez, J. App. Phys. **84**, 2459 (1998).
8. S.V.Koveshnikov and O.Kononchuk, App. Phys. Lett. **73**, 2340 (1998).
9. V.C.Venezia, D.J.Eaglesham, T.E.Haynes, A.Agarwal, D.C.Jacobson, H.-J.Gossmann, F.H.Baumann, Appl. Phys. Lett., **73**, 2980, (1998).
10. A.M.Mazzone, Phys. Stat. Sol. (a) **95**, 149 (1986).
11. J.F.Ziegler, J.P.Bierszack, U.Littmark, *The Stopping and Ranges of Ions in Solids* (Pergamon, New York, 1985).
12. R.Kalyanaraman, T.E.Haynes, V.C.Venezia, D.C.Jacobson, H.-J.Gossmann, C.S.Rafferty, appearing in App. Phys. Lett. V76, June, 2000
13. R.Kalyanaraman, T.E.Haynes, D.C.Jacobson, H.-J.Gossmann, C.S.Rafferty, 'Quantitative depth profiles of vacancy cluster defects produced by MeV ion implantation in Si: Species and dose dependence', these proceeding.
14. D.M.Follstaedt, S.M.Myers, G.A.Petersen, J.W.Medernach, J. Elec. Mat. **25**, 151 (1996).